tion-synchronous mode after the large damper has ceased its unidirectional motion. Figure 11 illustrates this.

Other techniques, such as combination fluid and ball dampers, suggest themselves as improvements to the basic circular constraint damper design. The particular application of the damper will determine the extent to which such improvements need be employed. In any case, Eqs. (4) and (5)—provided that the inequality (6) is obeyed—can be used in making preliminary damper performance estimates.

Appendix: Approximate Disk-Damper Equations of Motion

The exact equations were approximated by a set of simplified equations that embody only the principal terms. The variables appearing in the equations are defined in Fig. 6.

The angular rate $\dot{\varphi}$ defines the rotation rate of the transverse angular velocity vector $\boldsymbol{\Omega}_t$, that is, the departure of the actual nutation rate of the disk from the nominal rate Ω_{spin}/r. [It is the assumption of $\dot{\varphi} \equiv 0$ and $\varphi = 0$ in the following equations which leads to Eqs. (1) and (2) of the text.] The important lag angle δ is the displacement of the damper mass from its no-friction equilibrium position.

By ignoring the small variation in spin rate which occurs during damping and using only the principal terms of the exact equations, the following rather useful approximate equations are obtained:

$$\dot{\gamma} = -\frac{m\rho h}{I_T}\left(\frac{I_P}{I_T}\right)\Omega_s \sin\delta$$

$$\ddot{\alpha} + \frac{C_f}{m}\dot{\alpha} - \frac{h}{\rho}\left(\frac{I_P}{I_T}\right)^2 \Omega_s{}^2\gamma \sin\delta = -\frac{C_f}{m}\left(\frac{I_P - I_T}{I_T}\right)\Omega_s$$

$$\gamma\dot{\varphi} = -\frac{m\rho h}{I_T}\left(\frac{I_P}{I_T}\right)\Omega_s \cos\delta$$

$$\alpha \equiv \varphi - \delta$$

In Fig. 12 is shown a comparison of the γ vs time solutions using the exact equations and the approximate ones. The agreement that obtains in the fast damping or nutation-synchronous region is typical.

References

[1] Newkirk, H. L., Haseltine, W. R., and Pratt, A. V., "Stability of rotating space vehicles," Proc. Inst. Radio Engrs. **48**, 743–750 (1960).

[2] Haseltine, W. R., "Nutation damping rates for a spinning satellite," Aerospace Eng. **21**, 10–17 (March 1962).

[3] Cartwright, W. F., Trueblood, R. D., and Massingill, E. C., "Circular constraint nutation damper analysis," GM DRL Rept. TM 62-205, General Motors Corp. (December 1961).

JUNE 1963 AIAA JOURNAL VOL. 1, NO. 6

Hexagonal Cell Structures under Post-Buckling Axial Load

R. K. McFarland Jr.*

Jet Propulsion Laboratory, California Institute of Technology, Pasadena, Calif.

A method is presented for determining the approximate crushing stress of hexagonal cell structures subjected to axial loading. The purpose of performing this analysis was to determine an approximate analytical relation that can be used to compute the crushing stress of a given hexagonal cell structure. Of additional importance was the determination of the parameters that control the crushing stress and the sensitivity of the crushing stress to variations in these parameters. Experimental verification that was obtained for the resulting relations indicates that this method of analysis provides very effective upper and lower limits on the mean crushing stress of hexagonal cell structures. The purpose of the analysis was to provide rational means by which hexagonal cell structures can be designed for use as energy absorbers.

Nomenclature

A = basic panel element dimension
B = horizontal projection of basic panel element dimension
B_t = true length of B
D = width of cell wall
F = mean crushing stress
f = mean crushing force
K = P_w/D
M_{yp} = plastic moment per unit of length
P_w = width of basic panel element
q_{yp} = shear yield stress
S = cell minor diameter
t = cell wall thickness
U = energy
β = $(1 + 3\sin^2\theta)^{1/2}$
θ,ϕ = angles representing degree of collapse of a single cell element
ψ = angle representing shear deformation of a single cell element
σ_{yp} = tensile yield stress

Presented at the IAS Annual Summer Meeting, Los Angeles, Calif., June 19–22, 1962; revision received April 2, 1963. This paper presents the results of one phase of research carried out at the Jet Propulsion Laboratory, California Institute of Technology, under Contract No. NAS 7-100, sponsored by NASA.

* Research Engineer, Engineering Research.

I. Introduction

THIS report presents an upper-bound limit analysis of hexagonal cell structures subject to axial loading. The analysis is an approximate one, assuming a rigid-plastic material with equal yield stress in tension and compression and neglecting the effect of superimposed axial stresses on the yield criterion.

A simple mode of collapse for the hexagonal cell structure is assumed, based on experimental observations, and from this the collapse mechanisms are determined. The limit analysis techniques then are applied to the collapse mechanisms, and the energy of deformation is computed. The energy of deformation then is equated to the change in po-

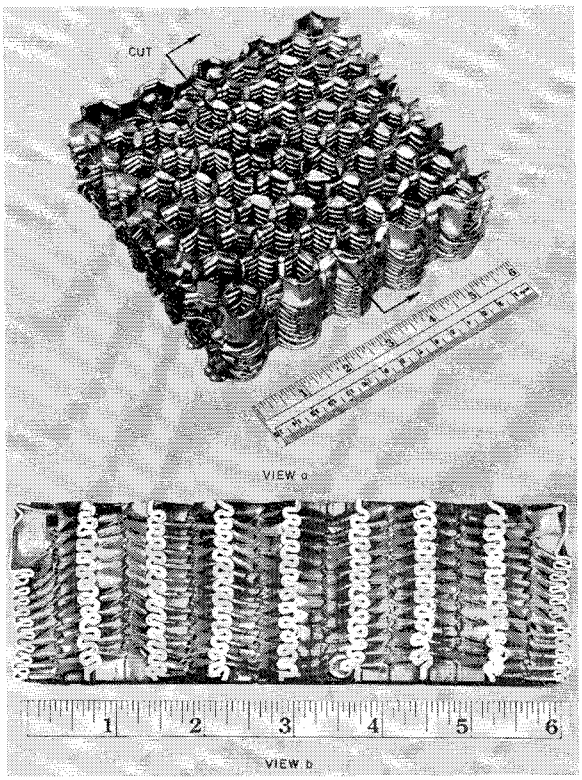

Fig. 1 Views of fully crushed hexagonal cell structure

tential energy of the applied force, and from this, a crushing force per unit area is obtained. The availability of these analytical relations allows a rational evaluation to be made of the efficiency of hexagonal cell structures as energy absorbers.

II. Energy of Deformation

On close examination of a crushed hexagonal cell structure, it is found that there is a definite symmetry to the collapse mode and that the collapse geometry is reproducible, as shown in Fig. 1. Unlike a thin cylindrical shell loaded axially, the collapse mode of the hexagonal cell is a function of the cell shape and geometrical constraints and does not change with variations of the cell-diameter to wall-thickness ratio for the range of this ratio considered in this analysis.

Once the basic mode of collapse is resolved, the mechanisms of collapse can be determined. By performing a limit analysis on the collapse mechanisms, the parameters that govern the collapse strength can be derived and expressed rationally.

To determine the crushing strength of the basic mode of collapse, an idealized model of this mode, shown in Fig. 2, was

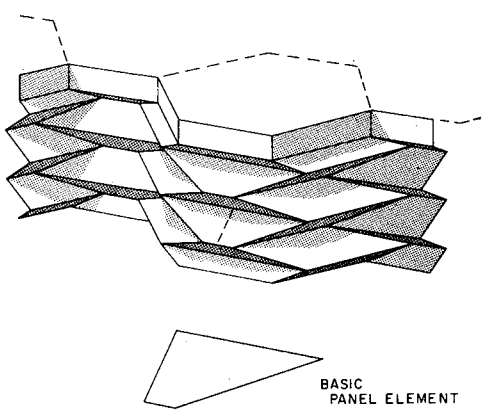

Fig. 2 Isometric projection of idealized mode of collapse of cell structure

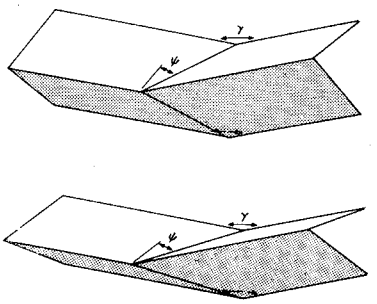

Fig. 3 Occurrence of in-plane shear deformation during crushing of hexagonal cell element

determined from experimental observation. It will be noted from Fig. 2 that the mode is symmetrical with respect to plate elements taken from the cellular structure. Because of geometrical constraints induced by adjoining cells in the complete cellular array, this mode is different from the mode that would be obtained from an individual hexagonal cell loaded axially.

Considering the collapse mechanisms of the idealized model, it is apparent that, in addition to the formation of a hinge mechanism along the fold lines, an in-plane deformation will have to occur to allow the model to collapse further. The need for this deformation is clarified in Fig. 3. In this cell element, the angle γ remains constant during crushing. For this deformation to continue, the angle γ would have to decrease or the angle ψ increase. The angle ψ can increase either by an in-plane shear deformation occurring in the panel elements or by a plastic rolling action occurring normal to and along the diagonal hinges. It is assumed that this action is accommodated by in-plane shear deformation; however, as will be discussed in Sec. IV, a certain amount of the plastic rolling deformation must occur with the shear deformation in order to obtain compatible deflections of the basic panel elements. On the basis of these assumptions, limit analyses were performed for a bending mechanism and a shear mechanism.

III. Energy of Bending Deformation

To perform a limit analysis on the bending mechanism, the idealized model is divided into identical basic elements, as shown in Figs. 2, 4, and 5. The energy of deformation incurred by one of the basic elements during the collapse of the model will be determined, and the results will be ap-

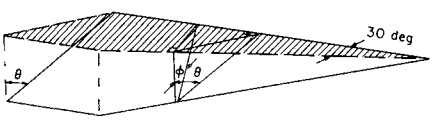

Fig. 4 Horizontal projection of partially rotated basic panel

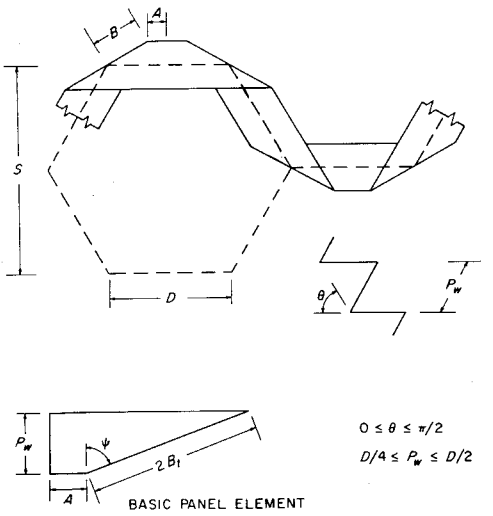

Fig. 5 Horizontal projection of cell structure

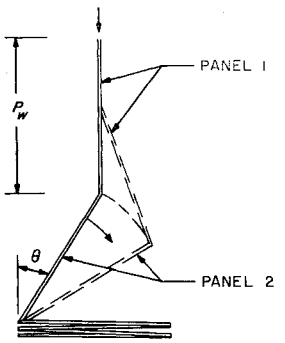

Fig. 6 Panel element rotations during crushing of hexagonal cell structure

plied to the composite model. It is necessary to define several relationships. Referring to Fig. 5,

$$D = S/3^{1/2} \tag{1}$$

$$A = \tfrac{1}{2}(D - 3^{1/2}P_w \sin\theta) \tag{2}$$

$$B_t = (P_w/2)(1 + 3\sin^2\theta)^{1/2} \tag{3}$$

and letting

$$\beta = (1 + 3\sin^2\theta)^{1/2} \tag{3a}$$

$$B_t = P_w\beta/2 \tag{4}$$

$$K = P_w/D \tag{5}$$

Note from Fig. 4 that, for an increment of deformation, two sides of the basic element rotate through an angle $\Delta\theta$, but the diagonal side will rotate through an angle $\Delta\phi$ for the same deformation. From Fig. 4, the relation between these two angles is

$$\tan\theta = (2/3^{1/2})\tan\theta \tag{6}$$

and

$$d\phi/d\theta = (3^{1/2}/2)(\cos^2\phi/\cos^2\theta) \tag{7}$$

Formulating the expression for the energy of bending deformation, let

$$dU_1 = M\Delta\theta$$

Then

$$M\Delta\theta = AM_{yp}\Delta\theta + [A + 2B\cos(\pi/6)]\Delta\theta + 2B_t\Delta\phi \tag{8}$$

Substituting Eqs. (1-7) into Eq. (8),

$$M\Delta\theta = \frac{S}{3^{1/2}} M_{yp}\left[1 + \frac{3^{1/2}}{2} K\beta\frac{\cos^2\phi}{\cos^2\theta}\right]\Delta\theta \tag{9}$$

To facilitate the integration of this expression, transform the variables $\Delta\theta$, ϕ, and θ to $\Delta\psi$ and ψ. From Fig. 5,

$$\cos\psi = P_w/2B_t$$

Using Eq. (4),

$$\cos\psi = \frac{1}{\beta} = \frac{1}{(1 + 3\sin^2\theta)^{1/2}} \text{ or } \sin\theta = \pm\frac{1}{3^{1/2}}\tan\psi$$

Since ψ increases as θ increases,

$$\sin\theta = (1/3^{1/2})\tan\psi \tag{10}$$

and from this relation,

$$\cos^2\theta = (3 - \tan^2\psi)/3 \tag{11}$$

and

$$d\theta = \sec^2\psi\, d\psi/(3 - \tan^2\psi)^{1/2} \tag{12}$$

Restating Eq. (6),

$$\tan\phi = (3^{1/2}/2)\tan\theta = (3^{1/2}/2)(\sin\theta/\cos\theta) \tag{12a}$$

Substituting Eqs. (10) and (11) in Eq. (12a),

$$\tan\phi = 3^{1/2}\tan\psi/2(3 - \tan^2\psi)^{1/2} \tag{13}$$

and from Eq. (13),

$$\cos^2\phi = [4(3 - \tan^2\psi)/(12 - \tan^2\psi)] \tag{14}$$

Substituting the relations expressed in Eqs. (11, 12, and 14) into Eq. (9),

$$dU_1 = M\Delta\theta = \frac{S}{3^{1/2}} M_{yp} \times \left[\frac{12\cos\psi - \tan^2\psi\cos\psi + 6\,(3^{1/2})K}{(13\cos^2\psi - 1)\,(4\cos^2\psi - 1)^{1/2}}\right] d\psi \tag{15}$$

Writing Eq. (15) in integral form,

$$U_1 = \frac{S}{3^{1/2}} M_{yp}\left\{\int_{\psi_1}^{\psi_2}\frac{12\cos\psi d\psi}{(13\cos^2\psi - 1)\,(4\cos^2\psi - 1)^{1/2}} - \int_{\psi_1}^{\psi_2}\frac{\tan^2\psi\cos\psi d\psi}{(13\cos^2\psi - 1)\,(4\cos^2\psi - 1)^{1/2}} + 6 \times 3^{1/2} K\int_{\psi_2}^{\psi_2}\frac{d\psi}{(13\cos^2\psi - 1)(4\cos^2\psi - 1)^{1/2}}\right\}$$

In terms of the limits of integration ψ_1 and ψ_2, the integrated result is

$$U_1 = \frac{S}{3^{1/2}} M_{yp}\left\{1.1547\tan^{-1}\frac{0.866\sin\psi}{(4\cos^2\psi - 1)^{1/2}} + \tan^{-1}\frac{(4\cos^2\psi - 1)^{1/2}}{\sin\psi} - \frac{2}{3^{1/2}}\tan^{-1}\frac{2(4\cos^2\psi - 1)^{1/2}}{3^{1/2}\sin\psi} - 4 \times 3^{1/2}K\left[-\frac{3}{4}\mathfrak{F}\left(\phi, \frac{3^{1/2}}{2}\right) + \frac{13}{12}\Pi\left(\phi, \frac{1}{3}\frac{3^{1/2}}{2}\right)\right]_{\psi_1}^{\psi^2}\right\} \tag{16}$$

where $\mathfrak{F}$ and Π refer to elliptic integrals of the first and third kind, respectively.

To establish the limits of integration for Eq. (16), it is necessary to consider the process of collapse of a hexagonal cell section. If an axial cut is taken through the wall of a partially collapsed cell unit, it is noted that only two basic panel elements will be subject to rotation at any given time, as illustrated in Fig. 6.

In collapsing a depth of P_w, panel 1 rotates from $\theta = 0°$ to $\theta = 30°$. Panel 2 rotates from $\theta = 30°$ to $\theta = 90°$. In terms of ψ, these limits would be as follows: panel 1, $\psi = 0°$ to $\psi = 40.89°$; and panel 2, $\psi = 40.89°$ to $\psi = 60°$. The integration could be performed in one operation; however, for later reference, the integration will be performed for each panel element.

Evaluating Eq. (16) with these limits of integration,

$$U_1 = (S/3^{1/2})M_{yp}\{[0.547 + 8.016K] + [1.509 + 4.381K]\}$$

where the two sets of brackets refer to panels 1 and 2, respectively.

Writing the combined results,

$$U_1 = (S/3)^{1/2}M_{yp}[2.057 + 12.396K] \tag{17}$$

This energy expression is equal to the mean crushing force times the distance over which it acts. To convert this to the mean crushing stress, it is necessary to determine the contributing area. Figure 7 represents a portion of a hexagonal cell structure.

As shown, two of the walls of each cell are of double thickness. This fact was not taken into consideration in the

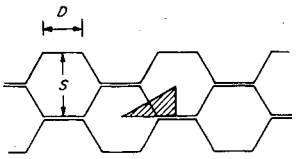

Fig. 7 Cross section of hexagonal cell structure illustrating area tributary to two basic panel elements

evaluation of the energy of deformation. It was assumed that there was no shear transfer between these walls during bending. The contributing area of two basic panel elements is

$$[3(3)^{1/2}/8]D^2$$

Recalling from conventional limit theory that the plastic hinge moment may be written in terms of the yield stress as

$$M_{yp} = (t^2/4)\sigma_{yp}$$

the foregoing two expressions may be substituted into Eq. (17) to obtain the mean crushing stress:

$$F = (4/3^{1/2})(\sigma_{yp}/K)\ (t^2/S^2)[2.057 + 12.396K]$$

or

$$F = (\sigma_{yp}/K)(t^2/S^2)[4.750 + 28.628K] \qquad (18)$$

IV. Energy of Shear Deformation

The limit analysis for the shear mechanism will be performed in the same manner used to determine the energy of bending deformation. It is necessary to determine the distribution of forces in the structure which produce in-plane deformations. Figure 8 is an exploded view of a partially crushed hexagonal cell section and indicates the most probable distribution of forces that exist due to axial loading. The forces are represented as point loads to simplify the visualization of their distribution in the structure. As noted in Fig. 8, the skewed side panels are subjected to a loading that would tend to induce in-plane shear deformations. The center panels are loaded in such a manner that no shear action could result from this loading condition. To maintain geometrical compatibility, if the side panels shear, the center panels also must change shape to conform to the new geometry. At this point, it is necessary to consider a refinement of the idealized model. In an actual specimen, as shown in Fig. 1, there are no sharp re-entrant angles and no ideal plastic hinges. At the intersections of the basic panel elements, relatively large radius bends and regions of plastically deformed material occur. Therefore, it is assumed that the incompatibility in geometry just mentioned will be satisfied by the complex deformations that occur in an actual specimen, and that shearing deformation will occur only in the side panels. The validity of this assumption is justified by experimental confirmation and a consideration of the force distribution on the center panels, as shown in Fig. 8.

Recalling the relations expressed in Eqs. (1–5 and 10), the shear deformation energy is computed in the following manner. Referring to Fig. 9, replacing the forces shown by equivalent shear forces, an expression then can be formulated

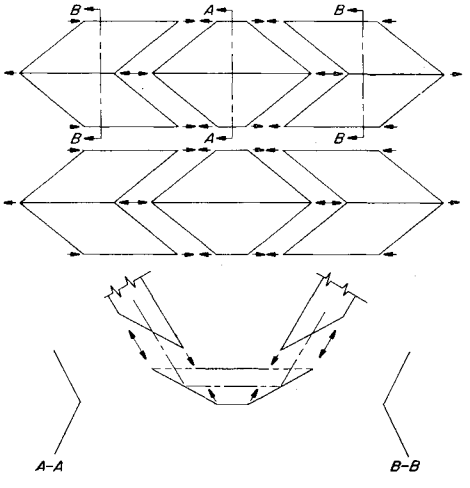

Fig. 8 Exploded view of cell model indicating forces causing in-plane deformation

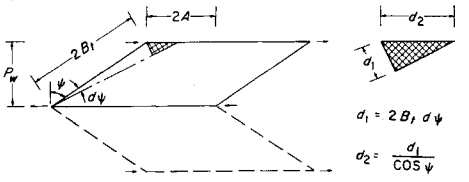

Fig. 9 Shear mechanism and corresponding parameters

for energy of deformation in terms of the shear yield stress. Hence,

$$dU_2 = g_{yp}t(2B_l \sin\psi + 2A)d_2 \qquad (19)$$

Performing the necessary substitutions,

$$dU_2 = q_{yp}t(P_w\beta \sin\psi + D - 3^{1/2}P_w \sin\theta)\ (2B_l/\cos\psi)d\psi$$

and

$$dU_2 = q_{yp}(tP_w^2 d\psi/K \cos^2\psi)$$

Since this value is for a configuration consisting of two basic panel elements, the energy increment per basic panel is

$$dU_2 = (q_{yp}tP_w^2/2K \cos^2\psi)d\psi \qquad (20)$$

As previously discussed, the integration is performed over two ranges of ψ, namely, $\psi = 0°$ to $\psi = 40.89°$, and $\psi = 40.89°$ to $\psi = 60°$. The basic panel elements must be formed before the shear deformation mechanism can occur. This requires that bending deformation mechanisms exist in the structure which define the basic panel elements before any energy will be absorbed in deforming these panels in shear. For rotations of $\psi = 0°$ to $\psi = 40.89°$, the basic collapse mode is not defined clearly. Rotations occur but are not large enough to form definite panel elements. Thus, the deformation resulting from this rotation can occur without the presence of a shear mechanism.

This occurrence would not follow for a true rigid-plastic material; however, because of the interaction of the two deformation mechanisms, it is necessary to consider this deviation from a rigid-plastic material to represent better the collapse mechanisms that occur in an actual specimen. Therefore, integrating the shear energy expression over only the range of $\psi = 40.89°$ to $\psi = 60°$,

$$U_2 = 0.433q_{yp}(tP_w^2/K) \qquad (21)$$

Equating this expression to the change in potential energy of the applied force,

$$U_2 = 0.433\ q_{yp}(tP_w^2/K) = fP_w$$

Equating this expression to the change in potential energy of the applied force,

$$U_2 = 0.433\ q_{yp}(rP_w^2/K) = fP_w$$

or

$$f = 0.433\ q_{yp}(tP_w/K)$$

The preceding expression represents the mean crushing force, and to convert this to the mean crushing stress, divide by the contributing area over which the force f acts:

$$F = 0.433\ q_{yp}\frac{tP_w}{K} \cdot \frac{8}{3(3^{1/2})D^2} = 1.155\ q_{yp}\frac{t}{S} \qquad (22)$$

V. Discussion of Result

If Eqs. (18) and (22) are combined, an expression representing the mean crushing stress of a hexagonal cell structure is obtained:

$$F = \sigma_{yp}\frac{t^2}{S^2}\left[\frac{4.750}{K} + 28.628\right] + 1.155\ q_{yp}\frac{t}{S} \qquad (23)$$

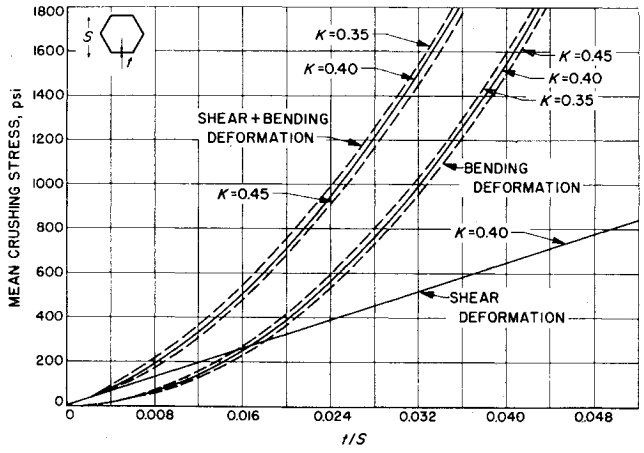

Fig. 10 Crushing stress vs t/S for 3003 H-19 aluminum hexagonal cell structure

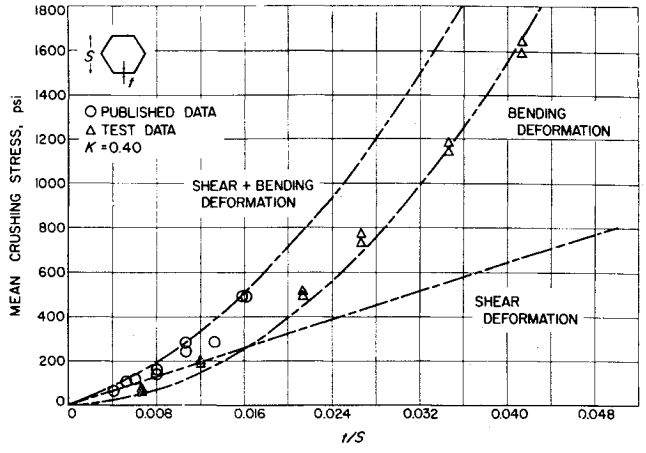

Fig. 11 Crushing stress vs t/S for 3003 H-19 aluminum hexagonal cell test specimens

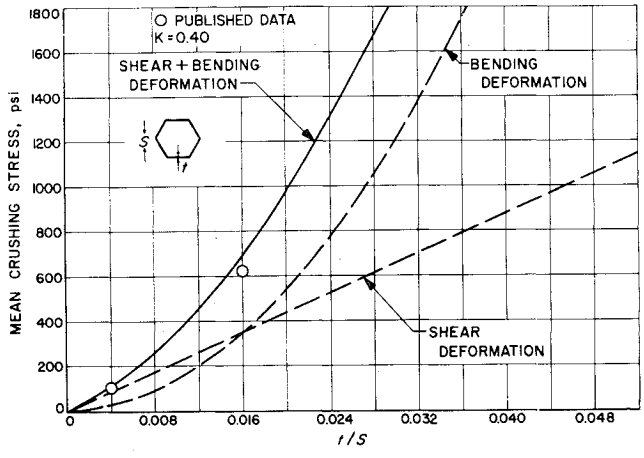

Fig. 12 Crushing stress vs t/S for 5052 H-39 aluminum hexagonal cell structure

The parameters that govern Eq. (23) are the properties of the material from which the cell structure is fabricated and the structural density of the cellular array. The material properties are represented by the yield strength in bending and in shear. The density of the cell structure is a function of the term t/S, which is the ratio of the cell wall thickness to the minor diameter of the cell. Thus, for a given cell diameter, the greater the wall thickness, the greater the crushing stress. One additional parameter occurs in Eq. (23): the term K. This term represents the ratio of one fourth of a buckling wavelength to the width of a cell wall. In the process of crushing, the phenomenon of buckling as commonly accepted does not occur. The crushing process is one of progressive collapse. Only during initial loading does a specimen become unstable and buckle, and this occurs for the first panel fold only. However, in crushing, the specimen continues to collapse in this same manner with the same panel depth as the first buckled panel. Based upon classical theory, the approximate value of K is 0.50; however, it has been found that, for the hexagonal cell structure, this value is very close to 0.40 for a wide range of t/S values.

The mean crushing stress as a function of t/S is plotted in Fig. 10, which indicates the lack of sensitivity of Eq. (23) to variations in K. For a $\pm 12\frac{1}{2}\%$ change in K, a change of approximately $\pm 4\%$ in mean crushing stress occurs; therefore, the mean crushing stress of a hexagonal cell structure is controlled, essentially, by the material properties and the structural density of the cellular array.

VI. Experimental Results

To obtain experimental confirmation of the preceding analysis, test data were obtained for commercially available hexagonal cell structures of 0.016 maximum density (i.e., t/S).[1] To supplement these data, a number of cell structures were fabricated from 3003 H-19 aluminum alloy with a minor cell diameter of 0.75 in. The wall thickness of the cell structure was varied to give t/S ratios in the range of presently available structures and in excess of this range. The results of the experimental program plus data taken from published reports are shown in Fig. 11. The results indicate a good upper-bound correlation for t/S values up to 0.016.

Data obtained from the test specimens indicate that the shear deformation energy is less than that assumed, particularly for increased values of t/S. The curve of bending deformation energy (Fig. 11) provides an effective lower bound for the mean crushing stress. It is apparent from Fig. 11 that the test data are consistently lower in value than published data. This, in part, is due to a scaling effect. The

[1] "Energy absorption properties of aluminum honeycomb," TSB-110, Hexcell Products Inc., Berkeley, Calif. (1960).

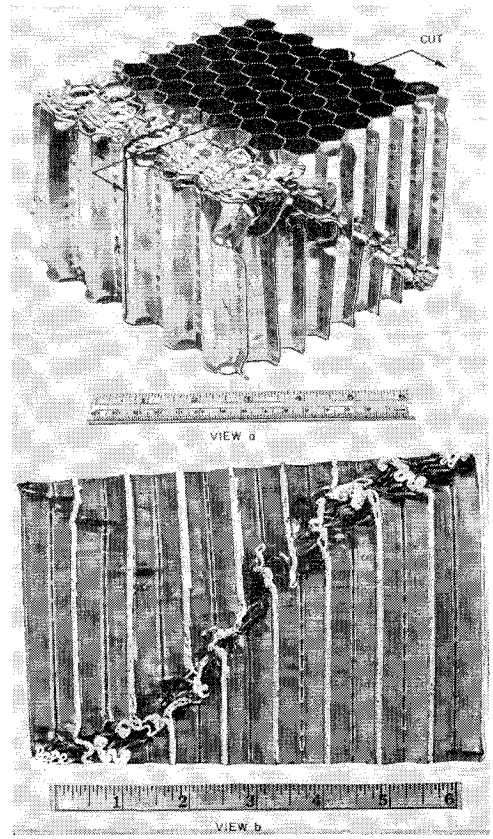

Fig. 13 Views of partially crushed hexagonal cell structure showing shear failure

specimens tested consisted of approximately square arrays of 78 cells with five partially unsupported cells on two sides of each specimen (Fig. 1). Thus, in these arrays, 12.8% of the cells were not constrained in the same manner as interior cells. If specimens with exterior dimensions twice the size of those tested had been used, only 6.8% of the cells in the array would have been partially constrained. No attempt was made to evaluate the magnitude of this scaling factor, because of the apparently small effect it had on the total crushing stress. A limited amount of published test data was obtained for a 5052 H-39 aluminum hexagonal cell structure, shown in Fig. 12 along with the derived relations using the 5052 H-39 material properties.

Of additional interest, it was found that there is an upper limit on the t/S ratio at which the hexagonal cell structure will collapse in a mode of failure that is entirely different from the mode normally observed. This failure mode is essentially a gross shear failure, as shown in the two views in Fig. 13. The t/S ratio for the test specimen at which this mode of failure begins to appear under static loading is approximately 0.040. The energy absorption of the shear mode is less than would be obtained by the crushing mode previously considered for corresponding t/S ratios. The emergency of the shear mode is controlled by the material properties and the t/S ratio.

VII. Conclusion

The foregoing analysis is presented as a first approach to the problem of determining the mean crushing stress of hexagonal cell structures. As previously stated, the purpose of this analysis was to derive a relationship for calculating the mean crushing stress and to determine the parameters that control it, with the end goal of providing a rational basis for the design of more efficient energy-absorbing structures. The method of analysis is a standard one, used to a large extent in structural analyses. There are a number of refinements to this theory, but no attempt was made to apply them because of the complex nature of the structure considered.

The results indicate a favorable correlation between theory and experiment for the limited amount of test data available. The use of higher yield stress materials, possessing adequate ductility, for the fabrication of the hexagonal cell structures would result in energy-absorbing properties well in excess of those exhibited by present-day aluminum-alloy cell structures.

Bibliography

Alexander, J. M., "An approximate analysis of the collapse of thin cylindrical shells under axial loading," Quart. J. Mech. Appl. Math. **XIII**, 10–14 (1960).

O'Bryan, T. C. and Hatch, H. G., "Limited investigation of crushable structures for acceleration protection of occupants of vehicles at low impact speeds," NASA TN D-158 (October 1959).

Pugsley, A. and Macaulay, M., "The large-scale crumpling of thin cylindrical columns," Quart. J. Mech. Appl. Math. **VIII**, 1–9 (1960).

"Impact deceleration systems applicable to lunar landing vehicles," Radioplane Rept. 2324, Van Nuys, Calif. (1960).

JUNE 1963 AIAA JOURNAL VOL. 1, NO. 6

Stretching of a Polar-Orthotropic Disk of Varying Thickness under Arbitrary Body Forces

CHARLES W. BERT* AND FRANCIS W. NIEDENFUHR†
Ohio State University, Columbus, Ohio

General equations are formulated for the elastic behavior of circular disks with radial variations of thickness and of polar-orthotropic elastic moduli and subject to any arbitrary systems of in-plane boundary or body forces. These equations are applied to and solved for an annular disk with a power-function variation in stiffness. The analysis is applicable to the design of turbine disks. Numerical results are obtained for the following examples of homogeneous disks rotating about eccentric normal axes: 1) an isotropic, uniform-thickness disk; and 2) a polar-orthotropic disk in which the thickness varies inversely with the radius.

Introduction

AMONG the earliest solutions of a plane elasticity problem involving nonsymmetric body forces is the analysis by Michell in 1900.[1] The first analysis of a varying-thickness disk subject to nonsymmetric generalized plane stress but no body forces was probably that of Shepherd,[2] who in 1933 treated a straight-tapered, rectangular-planform disk. Recently, Musick[3] and Conway[4] independently considered circular disks of hyperbolic profile subject to nonsymmetric boundary forces.

One of the first solutions for a circular disk under gravity loading in its plane was that of Michell.[1] In 1935 Biot[5] noted that body forces derivable from plane potential functions do not appear in the plane equilibrium equations. Circular disks with nonsymmetric body forces *not* derivable from potential functions, but derivable from more general functions, probably were analyzed first in 1938 by Mindlin,[6] who treated an eccentrically rotating, uniform-thickness disk. Apparently, varying-thickness disks subject to nonsymmetric body forces were treated first in 1952 by Vainberg,[7] who analyzed a disk rotating about a diameter.

Received by IAS October 26, 1962; revision received April 1, 1963. This paper is based on a dissertation presented by the first author to the Department of Engineering Mechanics of Ohio State University in August 1961, in partial fulfillment of the requirements for the degree of Doctor of Philosophy.

* Formerly Instructor, Department of Engineering Mechanics; now Program Director, Solid and Structural Mechanics Research, Battelle Memorial Institute, Columbus, Ohio. Member AIAA.

† Professor, Department of Engineering Mechanics.